A Facile Approach to Chemically Modified Graphene and its Polymer Nanocomposites

*Izzuddin Zaman, Hsu-Chiang Kuan, Qingshi Meng, Andrew Michelmore, Nobuyuki Kawashima, Terry Pitt, Liqun Zhang, Sherif Gouda, Lee Luong, and Jun Ma**

A scalable approach for the mass production of chemically modified graphene has yet to be developed, which holds the key to the large-scale production of stable graphene colloids for optical electronics, energy conversion, and storage materials, catalysis, sensors, composites, etc. Here, a facile approach to fabricating covalently modified graphene and its polymer nanocomposites is presented. The method involves: i) employing a common furnace, rather than a furnace installed with a quartz tube and operated in inert gas as required in previous studies, to treat a commercial graphite intercalation compound with thermal shocking and ultrasonication and fabricate graphene platelets (GnPs) with a thickness of 2.51 ± 0.39 nm that contain only 7 at% oxygen; ii) grafting these GnPs with a commercial, long-chain surfactant, which is able to create molecular entanglement with polymer matrixes by taking advantage of the reactions between the epoxide groups of the platelets and the end amine groups of the surfactant, to produce chemically modified graphene platelets (*m*- GnPs); and iii) solution-mixing *m*-GnPs with a commonly used polymer to fabricate nanocomposites. These *m*-GnPs are well dispersed in a polymer with highly improved mechanical properties and a low percolation threshold of electrical conductivity at 0.25 vol%. This novel approach could lead to the future scalable production of graphene and its nanocomposites.

1. Introduction

Although carbon nanotubes and silicate layers have been extensively studied over past decades, graphene is now hailed as the next generation of material for polymer nanocomposites. This is because electrically and thermally conducting graphene has the largest specific surface area, is stronger and stiffer than diamond, and, upon loading, can elongate a quarter of its length.[1–6] Recent studies have focused on oxidizing, exfoliating, functionalizing, and reducing graphene.[7–11] Reported methods for fabricating graphene, such as micromechanical exfoliation,[12] epitaxial growth,[13,14] and chemical vapour deposition,[15,16] are difficult to scale up for the fabrication of polymer nanocomposites. Recent methodologies include i) treating graphite with a harsh oxidation to produce graphite oxide with C:O ratios of ≈2:1, as in the Hummers method or its modified derivatives.[17,18] Graphite oxide can be expanded or even exfoliated in solvent by ultrasonication or rapid heating in inert gas. Notably, this method actually produces highly oxidized graphene that contains many irreversible defects and disorder, and shows little or no conductivity and highly reduced strength. Subsequent chemical reduction or thermal treatment recovers partial conductivity, albeit orders of magnitude below that of pristine graphene. In a typical procedure, graphite oxide is charged into a quartz tube in inert gas and then heated to temperatures over 1000 °C at high rates, such as 2000 °C min^{-1}.[19] The drawbacks of the reduction include: it is costly, owing to the presence of reducing chemicals or the special furnace equipped with a quartz tube and operated in inert gas; the reduction is never 100% complete and causes aggregation of graphene oxide in polymer matrixes; and the reduced graphene oxide exhibits a stiffness of 0.25 TPa, merely one fourth of its parent graphene.[20] In conclusion, this method is inappropriate for the scalable production of graphene. ii) A second recent method involves treating commercial graphite intercalation compounds by rapid heating to produce loosely stacked graphene platelets (GnPs) that can be further expanded in solvent by ultrasonication.[21,22] Each GnP, comprising a few or more graphene layers, ranges from 10–100 nm in thickness.[21–23] In spite of the high thickness, two advantages are

I. Zaman, Q. Meng, T. Pitt, S. Gouda, Prof. L. Luong, Dr. J. Ma
School of Advanced Manufacturing and Mechanical Engineering and Mawson Institute
University of South Australia
SA5095, Australia
E-mail: Jun.Ma@unisa.edu.au
I. Zaman
Faculty of Mechanical Engineering and Manufacturing
University of Tun Hussein Onn Malaysia
86400 Batu Pahat, Malaysia
Prof. H.-C. Kuan
Department of Energy Application Engineering
Far East University
Tainan County 744, Taiwan
Dr. A. Michelmore, Dr. N. Kawashima, Dr. J. Ma
Mawson Institute, University of South Australia
SA5095, Australia
Prof. L. Zhang
Key Laboratory for Nanomaterials
Ministry of Education
Beijing University of Chemical Technology
Beijing 100029, China

DOI: 10.1002/adfm.201103041

associated with this method: the starting-material graphite intercalation compounds are cost-effective as no harsh oxidation is involved, and the GnPs produced are of far lower oxidation degree than graphene oxide produced from method (i), implying no need for tedious reduction where dangerous, expensive chemicals are involved. Therefore, this method may hold potential for the mass production of graphene, although GnPs are generally perceived not to carry organic functional groups due to the thermal treatment.

Surface modification is crucial in producing a stable graphene colloid. As large fractions of hydroxyl, carbonyl, epoxy, and carboxylic groups are present on graphene oxide through acidification, three major types of methods have been developed to modify graphene oxide: i) transforming the carboxyl on graphene oxide edges into chlorides using $SOCl_2$, followed by reaction with amine-terminated surfactants;[24–26] ii) reacting graphene oxide with isocyanate;[27–29] and iii) bridging graphene oxide with surfactants through the reaction of the graphene oxide carboxylic groups with the surfactant amine groups.[30] These methods have been partially successful in modifying the graphene oxide surface: the first two methods, involving dangerous chemicals, are difficult for scaled-up production; and the bonding produced by method (iii) absorbs moisture in a humid environment. It is noteworthy that the reaction between the epoxide group of graphene oxide and the end amine group of surfactants has also been reported for the modification.[31–34] However, all of these methods start with highly oxidized graphite and short-chain surfactants, and this implies the necessity for reduction, which is inappropriate for the mass production of conducting graphene.

Forming nanocomposites is one of the major means of harvesting the striking mechanical and functional properties of graphene. Two major methodologies developed for fabricating polymer/graphene nanocomposites include solution mixing and in situ polymerization. Nanocomposites with up to a 10^4 increase in electrical conductivity have been fabricated by solution mixing.[35–40] Although robust mechanical performance is a prerequisite for the application of new materials, these nanocomposites have merely focused on conductivity rather than mechanical performance due to the lack of a reliable, cost-effective method for the modification of graphene for polymer nanocomposites. The interface between the dispersion layers and the matrix plays a crucial role in determining the structure and properties of nanocomposites, such as the improved mechanical properties of layered epoxy nanocomposites through interface modification using various surfactants.[28,41] In situ polymerization refers to polymerizing the mixture of monomer and suspended graphene platelets,[42,43] which promotes the dispersion and exfoliation of graphene. Two disadvantages are associated with this method: i) the low molecular weight, resulting in poor mechanical performance; and ii) the complexity, making them less compatible with industrial needs. From a fundamental viewpoint, it is indispensable to develop a general methodology for fabricating polymer/graphene nanocomposites via solution mixing, which is more compatible with industry practice than in situ polymerization.

In this study, we present a facile method for fabricating graphene platelets (GnPs) of ≈2.5 nm thickness, which can be covalently modified by a long-chain surfactant, in spite of the thermal treatment. The modified GnPs, possessing high C to O ratio, possess a highly improved capacity to form stable colloidal suspensions. Using the prepared graphene/epoxy nanocomposites as a model system, furthermore, we demonstrate that the resulting nanocomposites are electrically conductive and their mechanical performance is significantly improved.

2. Results and Discussion

2.1. Fabrication and Modification of Graphene Platelets

Inspired by a report where a thermal treatment of graphite oxide up to 727 °C produced a maximum quantity of epoxide groups,[44] we transferred a weighed commercial graphite intercalation compound (Asbury 3494, at 3–4 US$ lb^{-1}) directly into a crucible preheated at 700 °C, to produce a volume-expansion ratio of 283 times with an overall yield of 65% (**Figure 1**a,b). The loss was mainly caused by the compound's intercalates, which, during the thermal treatment, produced enormous gases for expansion. The simplicity of this method includes: i) the starting material is a cost-effective commercial product; ii) no further processing, such as oxidation, reduction, and washing, is involved; and iii) a common furnace is employed, rather than a furnace installed with a quartz tube and operating in inert gas as has been requested in previous reports.[19,45,46] The highly expanded product then experienced ultrasonication for further expansion to produce thinner graphene platelets (GnPs). Atomic force microscopy (AFM) measurements of randomly selected 20 platelets (Figure S1, Supporting Information) indicated a thickness of 2.51 ± 0.39 nm, much thinner than previous efforts of 10–100 nm.[21–23] Since thermal expansion has been reported to produce 1 nm-thick graphene oxide with a corrugated structure,[34] each GnP in this study, estimated from the thickness, may consist of 2–3 graphene layers. When the number of graphene layers increases from one to three, the Young's modulus remains nearly the same but the tensile strength reduces slightly from 130 GPa to 101 GPa,[47] indicating that GnPs can replace graphene in modifying polymers.

Starting from these much less oxidized graphene platelets (GnPs) (Figure 1b), we dispersed them at 0.5 vol% in seven solvents: acetone, tetrahydrofuran (THF), benzene, toluene, dichlorobenzene, *N,N'*- dimethylformamide, and *N*-methyl-2-pyrrolidone (NMP). While no clear difference was seen 30 min after sonication, as shown in **Figure 2**, leaving these vials for 4 h proved that NMP was best for suspending GnPs. Thus, NMP was adopted to modify GnPs using a commercial surfactant, polyoxyalkyleneamine, B200 (M_w = 2000 g mol^{-1}). The B200-modified GnPs are denoted as *m*-GnPs. The modification markedly improved the suspension of GnPs in solvent, since *m*-GnPs were able to be suspended in THF at 0.1 wt% for 7 d (Figure 1c) while GnPs remained suspended for 2 d (Figure 1b). When *m*-GnPs were dispersed in NMP, no precipitation was observed after at least five months of storage. This stable colloidal suspension of *m*-GnPs will provide a platform for a wide range of research and development of graphene-related products.

Transmission electron microscopy (TEM) (Figure 1d) and electron diffraction (ED) (Figure 1e) were used to characterize

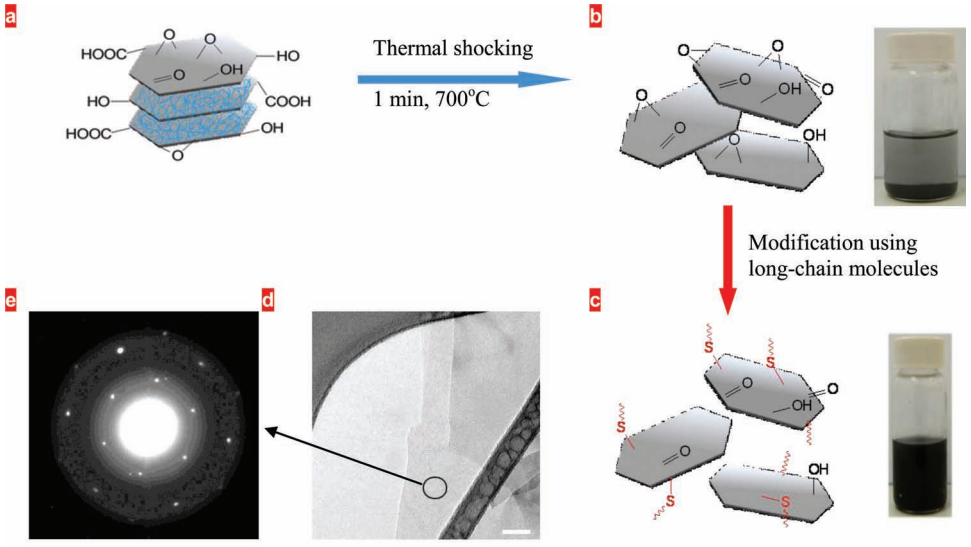

Figure 1. Fabrication of chemically modified graphene platelets (*m*-GnPs) from a commercial graphite intercalation compound. a) Schematic of graphite intercalation compound: "N" represents the intercalated molecules. b) Thermal shocking, to produce GnPs. c) Long-chain molecules grafting into GnPs: "S" represents a long-chain molecule. d) TEM image of a typical GnP suspended on a lacey carbon film-coated grid. The scale bar is 50 nm. e) Electron diffraction pattern of *m*-GnPs as in (d), showing high crystallization.

m-GnPs. In comparison with ED patterns of previous single graphene,[48,49] the ED pattern of our *m*-GnPs suggests a well-crystallized, 2–3 layered graphene structure, in agreement with the previously described AFM analysis. The key point for a maximum volume expansion is that the graphite intercalation compound must be transferred directly into a preheated crucible. This thermal shocking increased the C:O ratio from 88:12 to 93:7 (**Figure 3**a1,a2); it is noteworthy that this ratio, achieved without a quartz tube and inert gas, is higher than that of reduced graphene oxide.[46,50–55] Although combining thermal shock with ultrasonication has been reported to produce graphene platelets,[56] our approach has yielded the highest C:O ratio, implying the maximum retainment of functionality and mechanical performance from its parent graphene.

Through covalent functionalization, the ratio was reduced to 90:10 (Figure 3a3) due to the high C:O ratio of 2.9 of the grafted modifier. This process was further elucidated using Fourier transform IR (FTIR) spectroscopy. The absorption

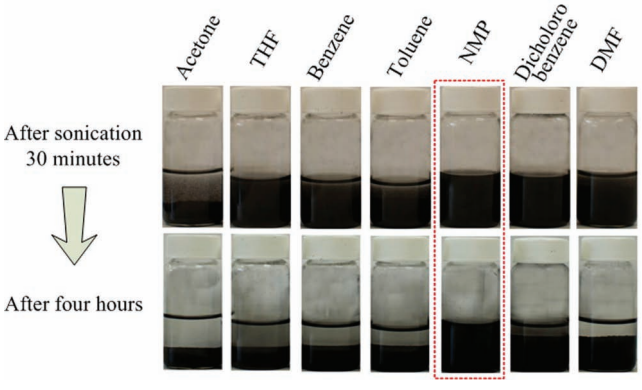

Figure 2. Dispersion of GnPs in seven organic solvents.

peaks of the epoxide groups at 1235 and 870 cm^{-1} increase obviously after the treatment (from Figure 3b1 to Figure 3b2), implying that more ether groups may be produced by the treatment. Once *m*-GnPs are thoroughly washed, a number of new absorption peaks appear, suggesting a new substance was grafted with GnPs (Figure 3b3). While the absorptions at 2980 and 2902 cm^{-1} represent the stretching vibration of the CH_2 groups,[57] the absorptions at 3677 and 1065 cm^{-1} correspond to the N–H and C–N groups of the B-200, respectively.[58] This proves that the B200 was grafted with GnPs, in agreement with the change of the C:O ratio (Figure 3a3). It is worth mentioning that the chemical bonding is stronger than the π-π physisorption of polymers on graphene.[59,60]

A series of experiments were designed to optimize the modification parameters. Of all the O atoms of the GnPs, we assume that 5 at% belong to epoxide groups that are capable of reacting with the amine-terminated surfactant. Tri-isopropanolamine was added as a catalyst to provide an alkaline environment. To promote the reaction, the numbers of moles of the surfactant and catalyst were doubled. Thus, we produced Recipe 1, where 0.1 g GnPs were mixed with 1.6 g surfactant and 0.15 g catalyst in 20 g NMP for reaction at 90 °C for 4 h. While keeping the GnP fraction and surfactant quantity fixed, we employed an orthogonal design to create five more recipes to identify the effect of the catalyst quantity, temperature, and time on the modification of GnPs (**Table 1**). These modified GnPs were investigated by FTIR spectroscopy (**Figure 4**). While no marked absorption is found for recipe 1, all others show obvious absorption. Since the recipe-4 product appeared to have the least intensity of the absorptions at y_1, y_2, and y_3, it is used as a benchmark to measure the absorption intensity of other products (Table 1). Recipe 6 indicates the most intensive absorption and thus was adopted to modify GnPs in this work. It is seen that the temperature and the ratio of the catalyst

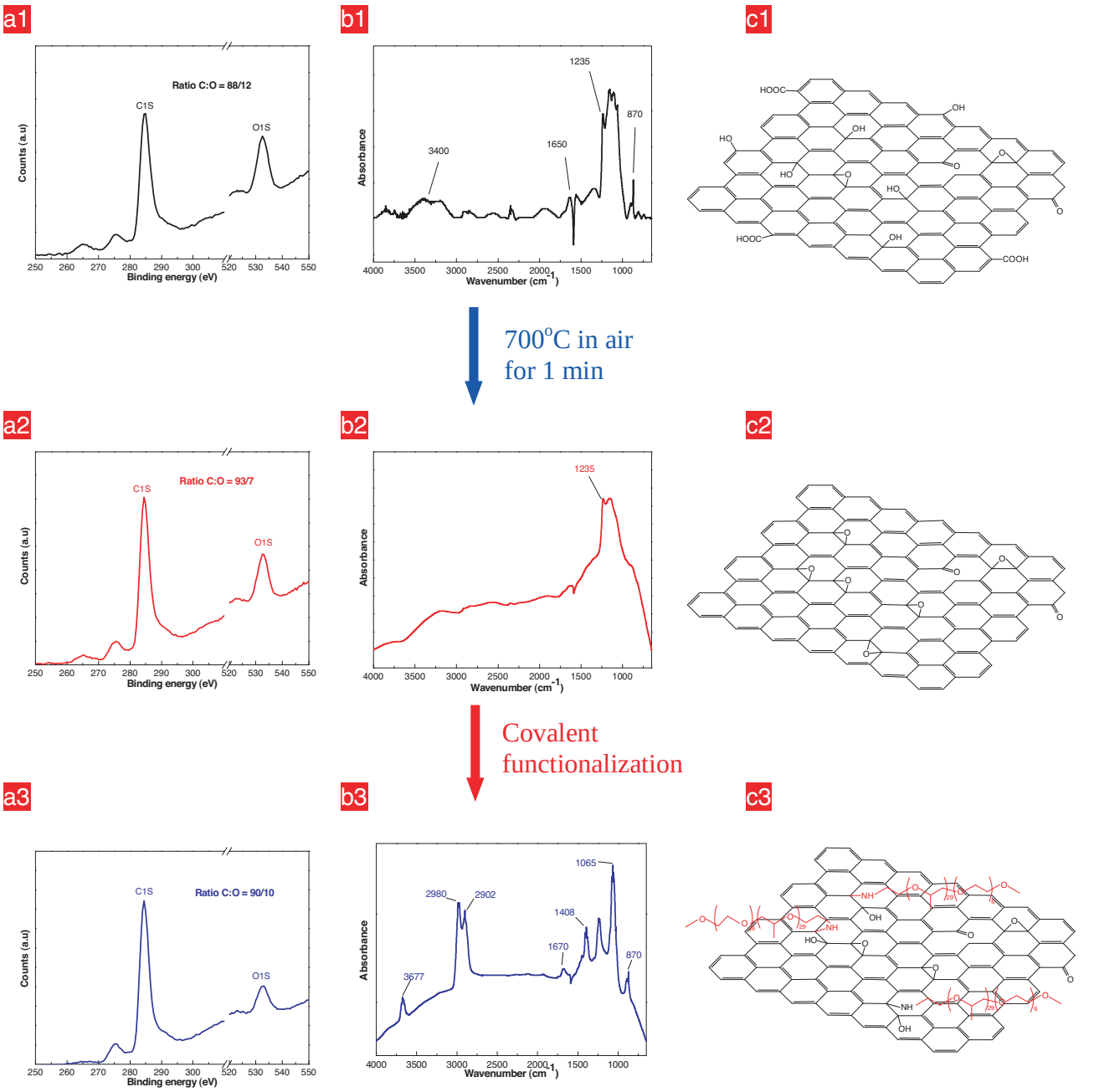

Figure 3. Fabrication and modification of chemically modified graphene platelets (*m*-GnPs). a1–a3) X-ray photoelectron spectroscopy (XPS) analysis for the washed graphite intercalation compound (GIC), GnPs, and *m*-GnPs. b1–b3) FTIR spectra of GIC, GnPs, and *m*-GnPs. c1–c3) Schematics of the atomic structures of GIC, GnPs, and *m*-GnPs.

to GnPs are the two major factors determining the grafting efficiency.

We propose schematic structures for the intermediate and final products of this approach (Figure 3c1–3c3). The raw material graphite intercalation compound was manufactured by treating highly crystalline, natural flake graphite with a mixture of sulfuric acid and certain other oxidizing agents which aided in "catalysis" of the sulfate intercalation, and the resultant product was a highly intumescent form of graphite (www.asbury.com). Upon thermal shock at 700 °C, these intercalates generated immense volumes of gases (CO_2, CO_2, H_2O, etc), which exceeded the van der Waals forces holding the graphite intercalation compound sheets together, leading to a high volume expansion. The washed compound is composed of hydroxyls (broad peak at 3050–3800 cm^{-1}), carbonyls (1750–1850 cm^{-1}), carboxyls (1650–1750 cm^{-1}), C=C (1500–1600 cm^{-1}), and ethers and epoxides (1000–1280 cm^{-1})[61–63] (Figure 3b1). The spectrum after the thermal treatment

Table 1. Recipes for producing chemically modified graphene platelets.

Recipe	Amount of catalyst [g]	Temperature [°C]	Time [h]	Relative y_1 intensity	Relative y_2s intensity	Relative y_3 intensity
1	0.15	90	4	N/A	N/A	N/A
2	0.15	150	12	1.5	1.4	1.7
3	0.46	90	12	1.3	1.4	1.3
4	0.16	150	1	1.0	1.0	1.0
5	1.38	90	1	1.5	1.5	1.6
6	1.38	150	4	2.6	2.4	2.6

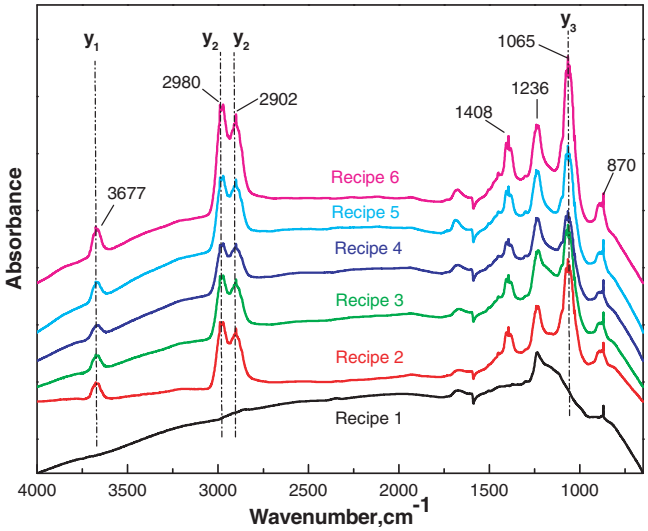

Figure 4. FTIR spectra of the modified GnPs produced by six recipes.

(Figure 3b2) indicates that most of the hydroxyl and carboxyl groups were removed. Importantly, the intensities of the bands assigned to the epoxides and ethers are obviously strengthened. Hydroxyl and carboxyl groups on the compound require lower temperatures for desorption than epoxy and carbonyl groups, as supported by a previous study where 63.5% of epoxide groups were found in graphite oxide when heat-treated at ≈700 °C.[44] During the subsequent modification, the epoxide groups of GnPs reacted with the long-chain surfactant, B200, as evidenced by the previously described FTIR spectroscopy analysis.

Figure 5a shows Raman spectra of thoroughly washed samples of graphite intercalation compounds, graphene platelets (GnPs), and chemically modified graphene platelets (*m*-GnPs). All samples show absorption at 1340 cm^{-1} and 1585 cm^{-1} corresponding to the D-band and G-band, respectively. However, the broadness and intensity of these absorption patterns are different. The D-band corresponds to the degree of disorder of the sp^3-hybridized carbon structure,[64,65] while the G-band is associated with in-plane vibrations of the sp^2-hybridized carbon atoms.[17,66] In general, the D-band intensity increases with the oxidation degree or the impurity quantity, while a high G-band intensity implies a regular graphene structure corresponding to good conducting properties and high strength. The D- to G-band ratio 0.54 of the graphite intercalation compound is much lower than that of graphite oxide in previous studies,[50–55,67,68] implying a low oxidation degree and defects. Upon thermal treatment, the ratio reduced from 0.54 to 0.07; this means that the intercalation compound can be reduced using a common furnace without a quartz tube running in inert gas. The decrease in the ratio is in agreement with the previously described X-ray photoelectron spectroscopy (XPS) analysis. The ratio increased markedly to 0.13 through the chemical modification, indicating the existence of B200 molecules on the graphene surface, in agreement with our XPS and FTIR analysis in Figure 3a3 and Figure 3b3, respectively.

The XRD spectra (Figure 5b) show a strong diffraction peak at 26.6°, fitting diffraction of the (002) plane with a 0.34 nm intergraphene spacing.[17,67] Although there is no obvious difference in the locations of the diffraction peaks, their intensities drastically reduce in the order: the intercalation compound > *m*-GnPs > GnPs, which is explained below. When thermally treated, the compound intercalants generated an immense volume of gases (CO_2, CO, H_2O, etc) that led to a pressure as high as 100 MPa.[45] The high pressure produced highly wrinkled GnPs with a volume expansion of over 200 times. This wrinkling may have started from aligned or adjacent functional groups, such as carbonyl and epoxide groups, causing a significant reduction in the diffraction intensity. When GnPs were modified, B200 with a few cycles of washing and separation rearranged and stacked these wrinkled GnPs, leading to an increased diffraction intensity.

C, H, and N elemental microanalysis gave the empirical formula of *m*-GnPs to be $C_{2.0}O_{0.08}H_{0.07}$–$(B200)_{0.004}$. This indicates that surface functionalization had taken place with a ratio of one B200 chain for approximately every 160 hexagonal cells of the graphene basal plane. Such a low ratio may explain why *m*-GnPs show a similar XRD diffraction angle to GnPs (Figure 5b).

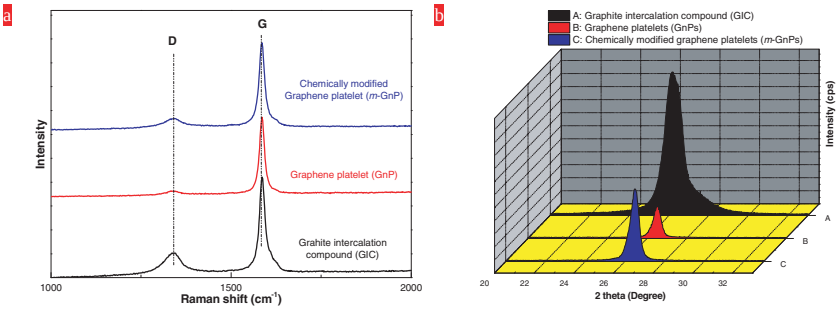

Figure 5. a,b) Evolution of Raman (a) and XRD patterns (b) of the washed graphite intercalation compound (GIC), GnPs and *m*-GnPs

2.2. Graphene/Epoxy Nanocomposites

In this study, we chose epoxy as a representative polymer due to its popularity in industries to fabricate polymer nanocomposites by solution compounding. The modified graphene platelets (*m*-GnPs) were suspended

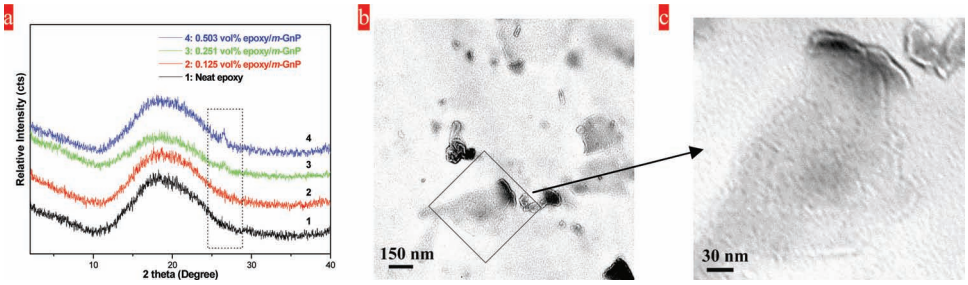

Figure 6. Structural characterization of graphene/epoxy nanocomposites. a) X-ray diffraction spectra of epoxy and its nanocomposites. b,c) TEM images of graphene/epoxy nanocomposites (0.244 vol%).

in THF and mixed with epoxy resin, followed by evaporating THF, mixing with a hardener, and curing. **Figure 6**a shows X-ray diffraction spectra of neat epoxy and its nanocomposites. The wide diffraction from 11 to 28° is caused by scattering of the cured epoxy molecules; although all nanocomposites show a similar diffraction pattern, a tiny shoulder peak is found at 26.6° for the 0.489 vol% nanocomposite, corresponding to an interlayer distance of 3.35 Å, which is associated with the graphitic plane. This implies that *m*-GnPs were possibly well-expanded, or even exfoliated, in epoxy. In the low-magnification TEM image in Figure 6b, *m*-GnPs are uniformly dispersed. Since graphene has a fairly similar composition to the matrix, the contrast between the dispersion particles and the matrix should be lower than that between clay and polymers.[69,70] Nevertheless, these highly crystalline graphene planes diffracted or scattered more transmission electrons than the polymer matrix, and thus appeared a little darker under TEM. Some much darker particles observed would have been caused by stacked graphene layers. At a higher magnification (Figure 6c), *m*-GnPs show little contrast with the matrix, which implies a low thickness—in agreement with the previous AFM measurements.

Figure 7 illustrates the electrical resistivities of the nanocomposites as a function of *m*-GnP volume fraction. The epoxy resistivity dropped by several orders of magnitude upon compounding with GnPs. At 0.244 vol%, the resistivity reduced by six orders of magnitude due to the formation of an electrically conductive network where a minimum distance between the filler-filler interaction must have reached. This percolation threshold is the lowest of all reported values for epoxy/graphene nanocomposites.[71–75] Our conductivities of epoxy and its nanocomposites were fitted by the power law model:

$$\sigma_C = \sigma_f (\psi - \psi_c)^t \quad (1)$$

In Equation 1, σ_c is the conductivity of nanocomposites, σ_f is the conductivity of the filler, ψ is the filler volume fraction, ψ_c is the percolation volume fraction and t is the critical exponent. The fitting line for the experimental results shown in the inset in Figure 7 corroborates well with the power law, resulting in $t = 2.15 \pm 0.59$, which is slightly lower than the experimental result reported by Stankovich et. al., 2.74 ± 0.2.[8]

While graphene is well known for its exceptionally high in-plane electrical conductivity, its through-plane conductivity is poor, which explains why its parent graphite is merely used as a semiconductor. As the number of graphene layers starts to pile up, their properties begin to approximate those of graphite. The formation of an electrically conductive network at such a low threshold leads to the following conclusions: i) these GnPs must uniformly disperse in the matrix and physically contact each other; ii) GnPs must be sufficiently thin to counter the side effects of their poor through-plane conductivity; and iii) GnPs can replace graphene in fabricating functional polymer nanocomposites due to their high performance and low cost.

The improvement in the mechanical and thermal properties (**Table 2**) also surpasses previous efforts in improving the Young's modulus,[22,76,77] fracture toughness and energy release rate,[78–80] and glass transition temperature of epoxy resins.[69–71] The reduction of the tensile strength and elongation at break is reasonable for stiff layered polymer nanocomposites, in agreement with previous research.[28,41] The grafting density of *m*-GnPs must be low, owing to the high C:O ratio of GnPs (Figure 3a2), and this ensures a high graphene structural integrity for retaining sufficient conductivity, stiffness, and strength. The high molecular weight of surfactant B200 provides a stable graphene colloid, leading to the fine dispersion of *m*-GnPs in the epoxy matrix. Therefore, these covalently modified, high C:O ratio GnPs have achieved

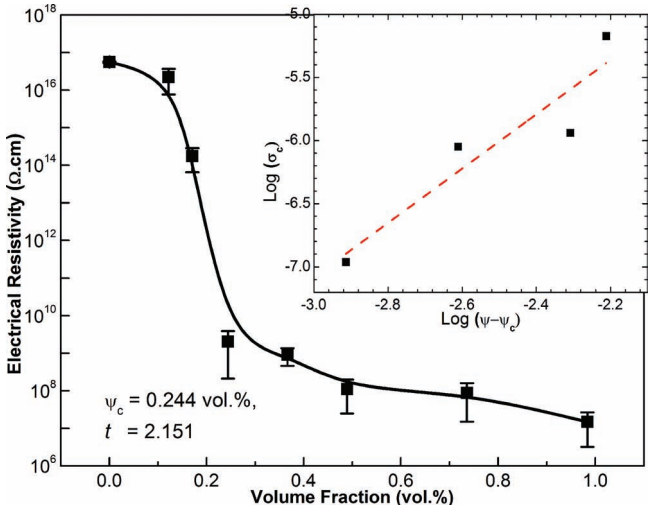

Figure 7. Electrical resistivity of epoxy and its graphene nanocomposites.

Table 2. Properties of neat epoxy and its nanocomposites cured by J230.

Materials	Young's Modulus [GPa]	Tensile strength [MPa]	Elongation at break [%]	Plane-strain fracture toughness, K_{1c} [MPa $m^{1/2}$]	Critical strain energy release rate, G_{1c} [kJ m^{-1}]	Glass transition temperature, T_g [°C]
Neat epoxy	2.692 ± 0.129	63.98 ± 2.14	5.31 0.29	0.657 ± 0.034	140.7 ± 7.9	83.4
0.122 vol% epoxy/graphene	2.992 ± 0.234	61.51 ± 1.49	4.01 ± 0.19	1.004 ± 0.033	295.6 ± 4.1	92.3
0.244 vol% epoxy/graphene	3.158 ± 0.089	51.44 ± 0.12	3.50 ± 0.11	1.258 ± 0.030	439.7 ± 8.8	90.0
0.489 vol% epoxy/graphene	3.412 ± 0.173	49.21 ± 2.94	2.68 ± 0.44	1.472 ± 0.023	557.3 ± 2.7	95.6

the previously described improvements in functionality and mechanical performance.

3. Conclusions

We have developed a facile, cost-effective approach for fabricating and modifying graphene. Our investigation showed that this method is indeed a general approach to make highly dispersed graphene/polymer nanohybrids with good control over the structure and properties. This is the first time that high-performace graphene/epoxy composites have been fabricated by solution-compounding a modified graphene with epoxy, which produced the lowest electrical conductivity percolation threshold for epoxy. Note that, with the same method, we also succeeded in making graphene/rubber nanocomposites. Therefore, our scalable synthesis of *m*-GnPs provides a platform to explore graphene for a wide range of applications.

4. Experimental Section

Materials: The graphite intercalation compound, Asbury 3494, was provided by Asbury Carbons, Asbury, NJ. The epoxy resin, diglycidyl ether of bisphenol A (DGEBA, Araldite-F), with an epoxide equivalent weight of 182–196 g per equiv., was purchased from Ciba–Geigy, Australia. THF and NMP were purchased from Sigma–Aldrich. The hardener, polyoxyalkyleneamine (J230), with M_w = 230 g mol^{-1}, was kindly provided by Huntsman (Singapore).

Graphene-Platelets Preparation: Our preparation started with transferring the graphite intercalation compound (Asbury 3494) into a preheated crucible at 700 °C in a common furnace, which was placed in the front of a fume cupboard to prevent nanoparticle inhaling hazard, and treating it for 60 s; a respirator, heat-resistant gloves, and safety glasses had to be worn in this process. As shown below, these expanded layers upon ultrasonication were able to disperse in solvent in the form of graphene platelets (GnPs).

Characterization of Graphene: AFM images were taken of GnPs using an NT-MDT scanning probe microscopy (SPM) instrument with NSG03 noncontact "golden" cantilevers. The samples were prepared by suspending GnPs in NMP at 0.0004 wt% for 30 min ultrasonication and then dropping the solution on a silicon wafer, followed by drying.

Graphene Modification: 0.1 g GnPs were dispersed in 20 g NMP in a metal container at 0.5 wt% by mechanical mixing for 10 min and ultrasonicating for 60 min. Since low-temperature sonication expands GnPs more effectively,[28] the temperature was set below 20 °C in this study. Based on Recipe 6 in Table 1, 1.6 g B200 surfactant and 1.38 g catalyst, tri-isopropanolamine, were added to the suspension, followed by mixing for 5 min using a mechanical mixer and ultrasonicating for 2 h. Then, the mixture was transferred into a round-bottom flask equipped with a condenser, and magnetically stirred for 4 h at 150 °C. The mixture was finally washed and filtered three times using acetone to remove NMP and excessive surfactant and catalyst. The B200-modified graphene platelets are abbreviated as *m*-GnPs.

Characterization of the Modified Graphene: We characterized our GnPs using a Philips CM200 transmission electron microscope (TEM) operating at an accelerating voltage of 200 kV. TEM samples were prepared by drying a droplet of the graphene suspension on a lacey carbon film. High-resolution XPS measurements were carried out using a SPECS SAGE XPS system with a Phoibos 150 analyser and an MCD-9 detector, which used non-monochromated Mg Kα radiation at 10 kV and 20 mA (200 W). The analysis spot size was circular with a diameter of 3 mm. IR spectra (700–4000 cm^{-1}) were measured using a Perkin–Elmer 65 FTIR spectrometer with a MIRacle single-reflection attenuated-total-reflectance (ATR) sample accessory. Raman spectra were recorded on a Renishaw inVia Raman microspectrometer with a 633 nm laser excitation. X-ray diffraction (XRD) was performed on the graphite intercalation compound, GnPs, and *m*-GnPs and their nanocomposites using a Diffraction Technology Mini-Materials Analyser (MMA). The diffractometer was equipped with curved graphite monochromators, tuned to Cu K radiation (λ = 1.5419 Å) with the tube voltage applied at 35 kV and 28.2 mA (1 kW). The diffraction patterns were collected in reflection-mode geometry for 2θ = 2–50° at a scanning rate of 1° min^{-1}.

Nanocomposite Preparation: A desired amount of *m*-GnPs was dispersed in THF at 1 wt% in a metal container by mechanically mixing for 10 min and ultrasonicating for 30 min at below 20 °C. A calculated quantity of epoxy (DGEBA, Araldite-F) was dissolved in acetone at 50 wt% by a similar protocol. Then, these two batches were mechanically mixed, followed by ultrasonication for 90 min at below 20 °C. Acetone and THF were evaporated by mixing and heating. When the mixture was cooled to 30 –35 °C, a hardener Jeffamine D 230 (J230) was added and mixed for 1 min. The final mixture was degassed, poured into a rubber mould, and heated at 120 °C for 12 h.

Nanocomposite Characterization: Tensile testing was performed on dumb-bell samples at 0.5 mm min^{-1} according to the American Society for Testing and Materials (ASTM) document D638 to obtain the elastic modulus, the ultimate stress, and the ultimate strain of neat epoxy and its nanocomposites. The average of each measurement was recorded from five repetitions. Young's moduli were calculated for a strain range of 0.05–0.15%. The compact-tension (CT) fracture toughness was tested in accordance with ASTM D5045 at 0.5 mm min^{-1}. By tapping a sharp razor blade, an instantly propagated crack was produced on each CT sample.[81] Glass transition temperatures were obtained using a Dynamic Mechanical Analyser 2980 (TA Instrument, Inc., USA) at 1 Hz. Rectangular samples were clamped using a single cantilever clamp with a supporting span of 20 mm and a torque of 1 N m, scanned from 50 °C to 180 °C, and recorded at 2 s per point. The volume resistivities of samples 6.8 ± 2.1 mm in thickness and 24 ± 0.2 mm in diameter were measured at room temperature using an Agilent 4339B high-resistivity meter equipped with a 16008B resistivity cell. The samples were tightly screw-pressed between two cylindrical electrodes that had a diameter of

26 mm. In order to provide stable values of the resistivity, the sample surface was finely polished to ensure a good electrical contact. The density of the graphene was taken as that of graphite, 2.26 g cm^{-3}; the matrix density was assumed to be 1.1 g cm^{-3}; thus, we were able to convert wt% to vol%.

Supporting Information

Supporting Information is available from the Wiley Online Library or from the author.

Acknowledgements

The authors thank B. Wade and J. Terlet for technical support at Adelaide Microscopy. J.M. thanks Asbury and Huntsman (Melbourne) for providing graphite intercalation compound and surfactant B200, respectively.

Received: December 15, 2011
Published online: April 10, 2012

[1] A. K. Geim, K. S. Novoselov, *Nat. Mater.* **2007**, *6*, 183.
[2] S. V. Morozov, K. S. Novoselov, M. I. Katsnelson, F. Schedin, D. C. Elias, J. A. Jaszczak, A. K. Geim, *Phys. Rev. Lett.* **2008**, *100*, 016602.
[3] C. Lee, X. D. Wei, J. W. Kysar, J. Hone, *Science* **2008**, *321*, 385.
[4] A. A. Balandin, S. Ghosh, W. Z. Bao, I. Calizo, D. Teweldebrhan, F. Miao, C. N. Lau, *Nano Lett.* **2008**, *8*, 902.
[5] A. K. Geim, *Science* **2009**, *324*, 1530.
[6] C. N. R. Rao, A. K. Sood, K. S. Subrahmanyam, A. Govindaraj, *Angew. Chem. Int. Ed.* **2009**, *48*, 7752.
[7] D. A. Dikin, S. Stankovich, E. J. Zimney, R. D. Piner, G. H. B. Dommett, G. Evmenenko, S. T. Nguyen, R. S. Ruoff, *Nature* **2007**, *448*, 457.
[8] S. Stankovich, D. A. Dikin, G. H. B. Dommett, K. M. Kohlhaas, E. J. Z. E. A. Stach, R. D. Piner, S. T. Nguyen, R. S. Ruoff, *Nature* **2006**, *442*, 282.
[9] Y. Zhu, S. Murali, W. Cai, X. Li, J. W. Suk, J. R. Potts, R. S. Ruoff, *Adv. Mater.* **2010**, *22*, 3906.
[10] X. Huang, X. Qi, F. Boey, H. Zhang, *Chem. Soc. Rev.* **2012**, *41*, 666.
[11] X. Huang, Z. Yin, S. Wu, X. Qi, Q. He, Q. Zhang, Q. Yan, F. Boey, H. Zhang, *Small* **2011**, *7*, 1876.
[12] P. W. Sutter, J. I. Flege, E. A. Sutter, *Nat. Mater.* **2008**, *7*, 406.
[13] K. V. Emtsev, A. Bostwick, K. Horn, J. Jobst, G. L. Kellogg, L. Ley, J. L. McChesney, T. Ohta, S. A. Reshanov, J. Röhrl, E. Rotenberg, A. K. Schmid, D. Waldmann, H. B. Weber, T. Seyller, *Nat. Mater.* **2009**, *8*, 203.
[14] K. S. Kim, Y. Zhao, H. Jang, S. Y. Lee, J. M. Kim, K. S. Kim, J. H. Ahn, P. Kim, J. Y. Choi, B. H. Hong, *Nature* **2009**, *457*, 706.
[15] X. S. Li, W. W. Cai, J. H. An, S. Kim, J. Nah, D. X. Yang, R. Piner, A. Velamakanni, I. Jung, E. Tutuc, S. K. Banerjee, L. Colombo, R. S. Ruoff, *Science* **2009**, *324*, 1312.
[16] X. Cao, Y. Shi, W. Shi, G. Lu, X. Huang, Q. Yan, Q. Zhang, H. Zhang, *Small* **2011**, *7*, 3163.
[17] J. Shen, H. Yizhe, M. Shi, X. Lu, C. Qin, M. Ye, *Chem. Mater.* **2009**, *21*, 3514.
[18] C. Gomez-Navarro, M. Burghard, K. Kern, *Nano Lett.* **2008**, *8*, 2045.
[19] H. C. Schniepp, J. L. Li, M. J. McAllister, H. Sai, M. Herrera-Alonso, D. H. Adamson, R. K. P. h. R. Car, D. A. Saville, I. A. Aksay, *J. Phys. Chem. B* **2006**, *110*, 8535.
[20] G. H. Chen, D. J. Wu, W. G. Weng, B. He, W. Yan, *Polym. Int.* **2001**, *50*, 980.
[21] A. Yasmin, J. J. Luo, I. M. Daniel, *Compos. Sci. Technol.* **2006**, *66*, 1182.
[22] Y. F. Zhao, M. Xiao, S. J. Wang, X. C. Ge, Y. Z. Meng, *Compos. Sci. Technol.* **2007**, *67*, 2528.
[23] A. Bagri, C. Mattevi, M. Acik, Y. J. Chabal, M. Chhowalla, V. B. Shenoy, *Nat. Chem.* **2010**, *2*, 581.
[24] G. L. Li, G. Liu, M. Li, D. Wan, K. G. Neoh, E. T. Kang, *J. Phys. Chem. C* **2010**, *114*, 12742.
[25] X. D. Zhuang, Y. Chen, G. Liu, P. P. Li, C. X. Zhu, E. T. Kang, *Adv. Mater.* **2010**, *22*, 1731.
[26] H. Kim, Y. Miura, C. W. Macosko, *Chem. Mater.* **2010**, *22*, 3441.
[27] Y. R. Lee, A. V. Raghu, H. M. Jeong, B. K. Kim, *Macromol. Chem. Phys.* **2009**, *210*, 1247.
[28] I. Zaman, T. T. Phan, H.-C. Kuan, Q. Meng, L. T. B. La, L. Luong, O. Youssf, J. Ma, *Polymer* **2011**, *52*, 1603.
[29] Y. Geng, S. J. Wang, J. K. Kim, *J. Nanosci. Nanotechnol.* **2008**, *8*, 6238.
[30] S. Park, D. A. Dikin, S. T. Nguyen, R. S. Ruoff, *J. Phys. Chem. C* **2009**, *113*, 15801.
[31] H. Yang, F. Li, C. Shan, D. Han, Q. Zhang, L. Niu, A. Ivaska, *J. Mater. Chem.* **2009**, *19*, 4632.
[32] H. Yang, C. Shan, F. Li, D. Han, Q. Zhang, L. Niu, *Chem. Commun.* **2009**, 3880.
[33] S. Wang, P.-J. Chia, L.-L. Chua, L.-H. Zhao, R.-Q. Png, S. Sivaramakrishnan, M. Zhou, R. G. S. Goh, R. H. Friend, A. T. S. Wee, P. K. H. Ho, *Adv. Mater.* **2008**, *20*, 3440.
[34] J. C. Meyer, A. K. Geim, M. I. Katsnelson, K. S. N. T. J. Booth, S. Roth, *Nature* **2007**, *446*, 60.
[35] K. Kalaitzidou, H. Fukushima, L. T. Drzal, *Compos. Sci. Technol.* **2007**, *67*, 2045.
[36] A. P. Yu, P. Ramesh, M. E. Itkis, E. Bekyarova, R. C. Haddon, *J. Phys. Chem. C* **2007**, *111*, 7565.
[37] S. Ansari, E. P. Giannelis, *J. Polym. Sci., Part B: Polym. Phys.* **2009**, *47*, 888.
[38] H. J. Salavagione, G. Martinez, M. A. Gomez, *J. Mater. Chem.* **2009**, *19*, 5027.
[39] M. T. Hung, O. Choi, Y. S. Jua, H. T. Hahn, *Appl. Phys. Lett.* **2006**, *89*, 023117.
[40] H. Fukushima, L. T Drzal, B. P. Rook, M. J. Rich, *J. Thermal Anal. Calorimetry* **2006**, *85*, 235.
[41] I. Zaman, Q. Le, H. C. Kuan, N. Kawashima, L. Luong, A. Gerson, J. Ma, *Polymer* **2011**, *52*, 497.
[42] M. Fang, K. Wang, H. Lu, Y. Yang, S. Nutt, *J. Mater. Chem.* **2009**, *19*, 7098.
[43] R. K. Layek, S. Samanta, D. P. Chatterjee, A. K. Nandi, *Polymer* **2010**, *51*, 5846.
[44] S. Niyogi, E. Bekyarova, M. E. Itkis, J. L. McWilliams, M. A. Hamon, R. C. Haddon, *J. Am. Chem. Soc.* **2006**, *128*, 7720.
[45] M. McAllister, J.-L. Li, D. H. Adamson, H. C. Schniepp, A. A. Abdala, J. Liu, M. Herrera-Alonso, D. L. Milius, R. Car, R. K. Prud'homme, I. A. Aksay, *Chem. Mater.* **2007**, *19*, 4396.
[46] K. S. Novoselov, A. K. Geim, S. V. Morozov, D. Jiang, Y. Zhang, S. V. Dubonos, I. V. Grigorieva, A. A. Firsov, *Science* **2004**, *306*, 666.
[47] C. Lee, X. D. Wei, Q. Y. Li, R. Carpick, J. W. Kysar, J. Hone, *Phys. Status Solidi B* **2009**, *246*.
[48] X. Li, G. Zhang, X. Bai, X. Sun, X. Wang, E. Wang, H. Dai, *Nat. Nanotechnol.* **2008**, *3*, 538.
[49] S. Park, R. S. Ruoff, *Nat.Nanotechnol.* **2009**, *4*, 217.
[50] M.-C. Hsiao, S.-H. Liao, M.-Y. Yen, P.-I. Liu, N.-W. Pu, C.-A. Wang, C.-C. M. Ma, *ACS Appl. Mater. Interfaces* **2010**, *2*, 3092.
[51] S. Stankovich, D. A. Dikin, R. D. Piner, K. A. Kohlhaas, A. Kleinhammes, Y. Jia, Y. Wu, S. T. Nguyen, R. S. Ruoff, *Carbon* **2007**, *45*, 1558.
[52] G. Wang, X. Shen, B. Wang, J. Yao, J. Park, *Carbon* **2009**, *47*, 1359.

[53] J. R. Lomeda, C. D. Doyle, D. V. Kosynkin, W.-F. Hwang, J. M. Tour, *J. Am. Chem. Soc.* **2008**, *130*, 16201.
[54] H. Wang, J. T. Robinson, X. Li, H. Dai, *J. Am. Chem. Soc.* **2009**, *131*, 9910.
[55] G. Wang, J. Yang, J. Park, X. Gou, B. Wang, H. Liu, J. Yao, *J. Phys. Chem. C* **2008**, *112*, 8192.
[56] B. Jiang, C. Tian, L. Wang, Y. Xu, R. Wang, Y. Qiao, Y. Ma, H. Fu, *Chem. Commun.* **2010**, 4920.
[57] H.-L. Guo, X.-F. Wang, Q.-Y. Qian, F.-B. Wang, X.-H. Xia, *ACS Nano* **2009**, *3*, 2653.
[58] S. J. R. Prabakar, S. S. Narayanan, *Anal. Bioanal. Chem.* **2006**, *386*, 2107.
[59] X. Qi, K.-Y. Pu, H. Li, X. Zhou, S. Wu, Q.-L. Fan, B. Liu, F. Boey, W. Huang, H. Zhang, *Angew. Chem. Int. Ed.* **2010**, *49*, 9426.
[60] X. Qi, K.-Y. Pu, X. Zhou, H. Li, B. Liu, F. Boey, W. Huang, H. Zhang, *Small* **2010**, *6*, 663.
[61] T. Szabó, O. Berkesi, I. Dékány, *Carbon* **2005**, *43*, 3186.
[62] E. Fuente, J. A. Menedez, M. A. Diez, D. Suarez, M. A. Montes-Moran, *J. Phys. Chem. B* **2003**, *107*, 6350.
[63] D. Hadži, A. Novak, *Trans. Faraday Soc.* **1955**, *51*, 1614.
[64] K. N. Kudin, B. Ozbas, H. C. Schniepp, R. K. Prud'homme, I. A. Aksay, R. Car, *Nano Lett.* **2008**, *8*, 36.
[65] V. Singh, D. Joung, L. Zhai, S. Das, S. I. Khondaker, S. Seal, *Prog. Mater. Sci.* **2011**, *56*, 1178.
[66] W. S. Kim, S. Y. Moon, N.-H. Park, H. Huh, K. B. Shim, H. Ham, *Chem. Mater.* **2011**, *23*, 940.
[67] H. Wang, Y. H. Hu, *Ind. Eng. Chem. Res.* **2011**, *50*, 6132.
[68] Y. Guo, C. Bao, L. Song, B. Yuan, Y. Hu, *Ind. Eng. Chem. Res.* **2011**, *50*, 7772.
[69] J. Ma, P. Xiang, Y. W. Mai, L. Q. Zhang, *Macromol. Rapid Commun.* **2004**, *25*, 1692.
[70] J. Ma, J. Xu, J. H. Ren, Z. Z. Yu, Y. W. Mai, *Polymer* **2003**, *44*, 4619.
[71] J. Liang, Y. Wang, Y. Huang, Y. Ma, Z. Liu, J. Cai, C. Zhang, H. Gao, Y. Chen, *Carbon* **2009**, *47*, 922.
[72] H. G. Tang, Q. Qi, Y. P. Wu, G. H. Liang, L. Zhang, J. Ma, *Macromol. Mater. Eng.* **2006**, *291*, 629.
[73] N. Jovic, D. Dudic, A. Montone, M. V. Antisari, M. Mitric, V. Djokovic, *Scr. Materialia* **2008**, *58*, 846.
[74] A. Celzard, E. McRae, J. F. Mareche, G. Furdin, M. Dufort, C. Deleuze, *J. Phys. Chem. Solids* **1996**, *57*, 715.
[75] L. L. Wu, X. Lv, C. C. Zhang, *Adv. Mater. Res.* **2011**, *239*, 55.
[76] J. Li, M. L. Sham, J. K. Kim, G. Marom, *Compos. Sci. Technol.* **2007**, *67*, 296.
[77] A. Yasmin, I. M. Daniel, *Polymer* **2004**, *45*, 8211.
[78] M. A. Rafiee, J. Rafiee, Z. Wang, H. Song, Z.-Z. Yu, N. Koratkar, *ACS Nano* **2009**, *3*, 3884.
[79] S. Q. Li, F. Wang, Y. Wang, J. W. Wang, J. Ma, J. Xiao, *J. Mater. Sci.* **2008**, *43*, 2653.
[80] S. Jana, W. H. Zhong, *Mater. Sci. Eng. A* **2009**, *525*, 138.
[81] J. Ma, Q. Qi, J. Bayley, X. S. Du, M. S. Mo, L. Q. Zhang, *Polym. Testing* **2007**, *26*, 445.